EDUCATUM JSMT Vol. 6 No. 2 (2019)
ISSN 2289-7070 / eISSN 2462-2451 (22-34)
https://ejournal.upsi.edu.my/index.php/EJSMT/index

Structure and Physical Properties of $30MgSO_4$-(70-x) P_2O_5-xSm_2O_3 glasses

Aliyu Mohammed Aliyu[1*], N.E Ahmed[2]

[1]Department of physics, Faculty of Sciences, Bauchi State University, Gadau, Bauchi Nigeria
[2]Department of physics, Faculty of Sciences, University Technology, Johor Bahru, Malaysia

*Corresponding author: aliyualiyuphy@gmail.com

DOI: https://doi.org/10.37134/ejsmt.vol6.2.3.2019

Received: 18 August 2019; Accepted: 10 December 2019; Published: 15 December 2019

Abstract

Glasses in the series $30MgSO_4$-(70-x) P_2O_5-xSm_2O_3 $0.2 \leq x \leq 1.0$ mol percent were prepared by single step melt-quench techniques, the structure, physical and optical properties of samarium oxide at different concentrations were studied. The amorphous phase of the samples was verified by X-ray diffraction spectroscopy, the structural units were investigated using Fourier Transform Infrared, Raman and NMR spectroscopy where the spectra reveal the presence of symmetric, asymmetric, torsoional and bending vibration of phosphate groups, the NMR spectra reveals the changes in Q^n distribution here discussed, the compositional dependence on physical (density, average molar weight, dielectric constant, Inter-nuclear distance, Field strength, Molar volume, Molar refractivity etc) and optical parameters were determined. In terms of structural modifications, there is variation of density and molar volume, the glass sample has increasing refractive index values with decreasing molar volume content. The luminescence spectra were observed within UV-Vis-NIR region, the absorption spectra of the sample were recorded in the range of 350 to 1800 nm meanwhile, absorption edge the optical band-gap, and ΔE was evaluated. Our result may be advantageous for many optical applications (e.g visible lasers or color displays).

Keywords: Melt-quench, Ultra-phosphate, Spectroscopy, Luminescence, Density

INTRODUCTION

With increasing demand of energy and the resulting outlays, there is a crucial need for the energy saving devices. Therefore, a consideration has to be given in many optical devices such as LEDs, solid state laser or any optical devices so as to replace/assist the conventional lightning. The glasses have wide range of applications in modern science and technologies among which phosphate based glasses has some advantages over the conventional silicate and borate glasses due their good glass forming ability [1], its posses high transparency, high gain density, low melting and softening temperature [2] with favorable solubility of rare earth ions [3] and used for verifications of certain nuclear wastes [4, 5]. The hygroscopic nature of the phosphate glasses was verified by the spectroscopic absorption bands due to hydroxyl groups been observed at certain range [6-9], the hygroscopic character leads to the weaker chemical stability and devitrification tendencies [10] which can't be protected adequately, the addition of modifier oxides help to overcome these difficulties. Preparation of phosphate based glasses in the ultra- meta- and poly-phosphate region have been achieved [2, 11, 12] using some amounts of modifier oxides such as Na_2O [2] Ca-O [11] or Mg-O [12, 13]. Two competing modifier and intermediate oxides were combined in the glass system to modify and stabilized the phosphate structure with relatively lower amount. Even though, some report shows that the binary Magnesium phosphate (MgO-P_2O_5) glasses exhibit anomalous behavior near the Q^2 units [12, 13], this behavior attributed to change in physical properties of glasses which has been observed in relation to MgO coordination number. Furthermore, magnesium oxides can help in reducing the hygroscopic nature of host glasses [15] incorporation of sulfur results in structural modification of phosphate structure [16] as sulfur ions are widely dissolve in the P_2O_5 glass and

mostly remain as isolated units, for glasses with sulfo-phosphate ratio 1:2 the glass structure is entirely de-polymerized [17]. The spectroscopic and physical properties of tellurite, borate, silicate and phosphate glasses doped with various quantities of rare earth ions have been investigated previously[18, 19]. These ions incorporated with host materials increases their potential application in fabrication of optical fibers, memory devices, optoelectronics due to sufficient absorption and emission band obtained between the energy levels [20, 21]. Samarium oxides is among the most interesting rare earth ions doped glasses that exhibit a strong fluorescence within a visible region having a weaker concentration quenching and no up-conversion losses been used for laser materials [18] for hole burning studies [22] color display [23] and are fit to analyze the energy transfer processes. The present work is aimed to prepare and study the Sm^{3+} -doped magnesium sulfate ultra-phosphate glass with different samarium oxide concentration and its effect on physical and optical properties.

EXPERIMENTAL

Samples preparation

A series of Sm^{3+} -doped magnesium sulfate ultra-phosphate glasses of type 30$MgSO_4$-(70-*x*) P_2O_5-*x*Sm_2O_3 with $0.2 \leq x \leq 1.0$ mol % (referred to as MSPSm) were prepared by single step conventional melt quench method. The appreciable amount of reagent grade $MgSO_4$, H_2PO_4 and Sm_2O_3 weighed by digital electronic balance with a certified accuracy of $\pm$ 0.001 g of 99.8 % purity were mixed thoroughly for 20g batches. The samples preheated in an alumina crucible at 300 ℃ for 45 min, then transferred to electric furnace of higher temperature at 1200 ℃ for an hour, the samples was stirred occasionally to ensure homogenization and to obtained bubbles free. The samples were then poured directly on to a rectangular stainless steel plate and annealed for 5hours in order to eliminate the internal stress and preserved the melt in desiccators for further characterization. Samples of required optical quality were then selected, grinded and polished for spectroscopic properties, the chemical transformation equations of the substances preheated at 300 ℃ were indicated as:

Magnesium sulfide: $MgS + H_2SO_4 \rightarrow MgSO_4 + H_2S \uparrow$,
Phosphoric acid: $2H_3PO_4 \rightarrow P_2O_5 + 3H_2O \uparrow$,

Instrumentation

X-ray measurement

In the present study, the materials phase was determined using X-ray diffraction technique recoded at angle 2 theta in the range of $10° \leq \theta \leq 80°$ with scanning rate of 2.4°/min. The samples were examined with a diffraction software analysis of wavelength (Cu Kα, λ= 1.54056 Å) operating at 40 kV, 30 mA at room temperature. The broad hump centered at around 18-20° (=2θ) without any sharp band this verify the amorphous state of materials.

Density - molar volume measurement

The density (ρ) of each sample were discovered by Archimedes and principle, the samples weighted in air and submerge in toluene of densities 0.865 g/cm^3, and are calculated using

$$\rho(g/cc) = \frac{w_a}{w_a - w_t}\rho_t \quad (1)$$

where W_a and W_t is the weight of glass samples in air and that of toluene and ρ_t is density of toluene, all sample weight measurements were made using a digital balance. The corresponding molar volume

were obtained using the relation V_m = M_t/ρ (cm^3/mol) as M_t is the total molar weight of the samples and ρ is the density in equation (1), the experiment was repeated four times and take the average values.

Refractive index measurement

Refractive index (n) is the parameter used to determine the suitability for optical materials which are demonstrated using the subsequent equation (2) where Eg is the optical band gap obtained from the absorption measurement.

$$\frac{n^2-1}{n^2+2}=1-\sqrt{E_g/20}$$

(2)

Optical absorption measurement

The optical absorption spectra of bulk samples were determine in the range of 350-1800 nm (wave length) by double beam spectrophotometer at room temperature (Figure 7). The measurement made by Shimadzu 3101 PC UV-Vis-NIR Spectrophometer located at Thin Film Laboratory in Physics Department of University Technology Malaysia. The molar absorption coefficient $\alpha(v)$ was evaluated using the Lambert-Beer law as [11, 24].

$$\alpha(v)=\left(1/D\right)\ln\left(l_o/l_t\right)$$

(3)

where D is the thickness of the samples and I_0 and I_t are the corresponding intensities of incident and the transmitted radiations respectively.

FTIR, Raman and NMR spectroscopy

The IR absorption spectra were measured to study the structural behavior of the glass samples over a specific frequency range 400-1400 cm^{-1} obtained by employing potassium bromide (KBr) pallet technique of about 1:100 ratio to form a thin pellet. The pressure gauge of 5 tons cm^{-2} for five minutes to yield a transparent pallet of ~0.5 mm thickness ready for mounting in the IR spectrophotometer (Perkin-Elmer 1710 FT-IR spectrophotometer). Raman spectra of the samples was still measured at room temperature with Raman X-plora spectrometer over a wave number range 200-2000 cm^{-1} and Neodymium Yttrium Aluminum Garnet (Nd:YAG) as laser source for 600-1200 nm grating. The solid-state ^{31}P MAS NMR spectra (Figure 4) were obtained by Brucker Advance III HD at high-resolution power of 400 MHz (magnetic field 9.4 T), 16 µs pulse at recycle time of 2.5 sec with spinning speed of 14 kHz, at constant frequency of phosphorus 161.94 MHz. The entire chemical shift was expressed in parts-per-million (ppm) relative to 85% aqueous phosphate acid.

RESULTS AND DISCUSSION

Structural properties

X-Ray Diffraction Analysis

The X-ray diffraction pattern of the glass samples 30MgSO$_4$– (70-*x*) P$_2$O$_5$-*x*Sm$_2$O$_3$ in mol % (Figure 1), there is no sign of devitrification tendencies in the glass system, this indicate that the samples are amorphous in nature, from the spectra obtained there is absence of sharp peaks, it's lacks long-range order as presented in the previous literature [10, 11].

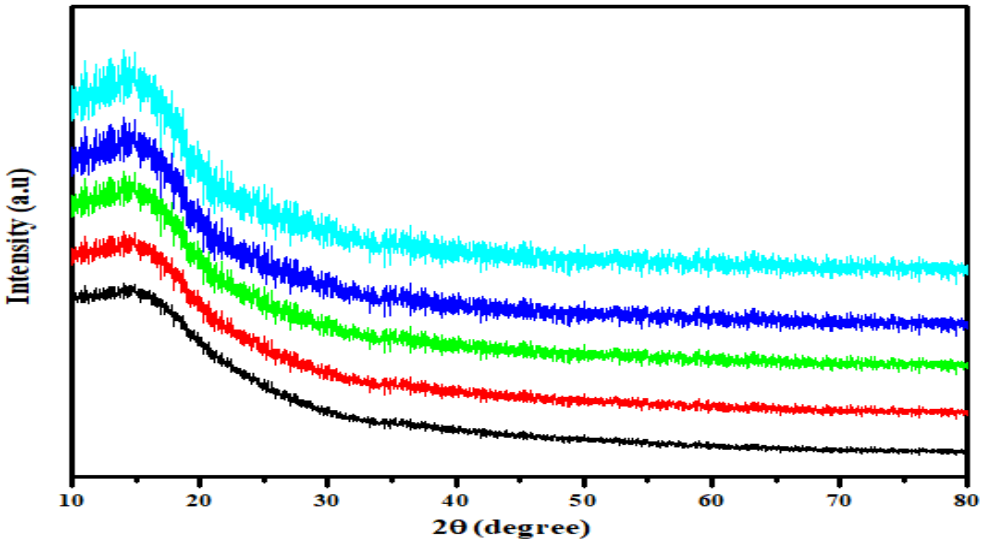

Figure 1 XRD pattern of MSP; Sm glasses

Infrared Spectra Analysis

The spectra (IR) of 30MgSO$_4$-(70-*x*) P$_2$O$_5$-*x*Sm$_2$O$_3$, with $0.2 \leq x \leq 1.0$ mol% glasses as shown in Figure 2, the common features of the IR spectra of v-P$_2$O$_5$ glass are vibrations around 1640 cm^{-1} assigned to bending vibration of hydroxyl group [25, 26] a partially bound water. The characteristic feature for stretching vibration of terminal bond (P=O) at about 1274 cm^{-1} [25, 27] are in Q^3 region, the vibration around 1083 cm^{-1} assigned to $(PO_3)^{2-}$ in the meta-phosphate region [25,28], the region at about 860–940 cm^{-1} were assigned to asymmetric stretching of P-O-P link, ν_{as} (P-O-P) [27,28] in Q^2 region, while the band at about 750-810 cm^{-1} have been identified as the symmetric stretching modes of P-O-P units of bridging oxygen link [25, 26] in Q^2 chain, the observed band at ~514 cm^{-1} attributed to bending modes of δ(PO) group [29,30].

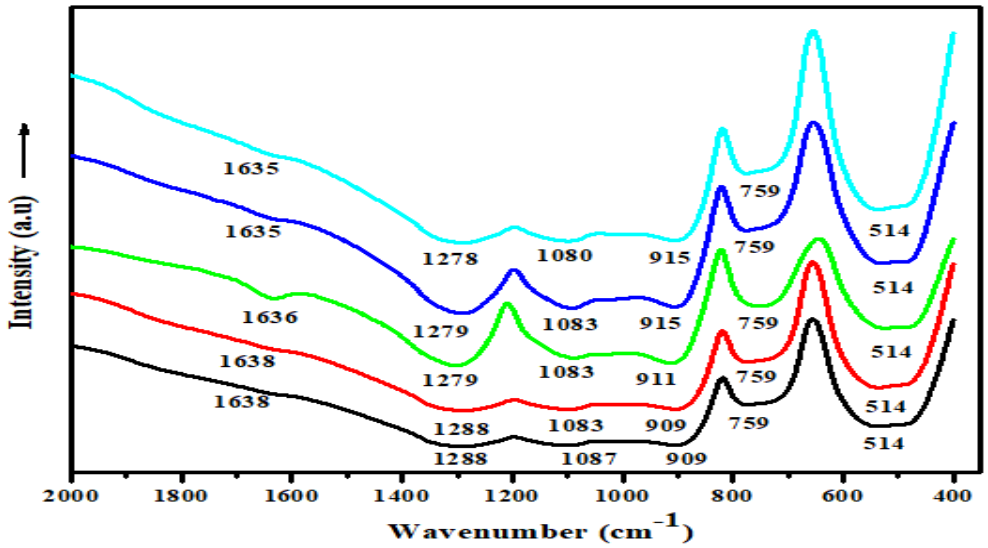

Figure 2 IR spectra for MSP; Sm glasses

Raman Spectra Analysis

Figure 3 shows the Raman spectra of phosphate based glass samples in the region of 200 to 1500 cm^{-1}, the shape of the Raman Spectra goes along with those found in literature, exhibiting various phases of symmetric (v_s) and asymmetric (v_s) vibrational modes due to predominant covalence of PO_4, PO_3, PO_2 and P-O [31**]** group, small positions of bands in sulfate overlapped with phosphate units demonstrating tendencies of inter cluster covalent-ionic interactions between phosphate and sulfate groups. In both spectral responses (Raman and IR) on phosphate network activities are based on bending modes, $v \sim 500$ cm^{-1}, NBOs modes, $v \sim 940 - 1380$ cm^{-1} and bridging oxygen modes, $v \sim 700 - 900$ cm^{-1}[32]. The structural changes were observed as a result of modifier addition in the phosphate glass matrix and the characteristic features of the host network are basically restricted to the higher wave number positions of the spectra (300–1400 cm^{-1}) and are corresponding to the vibration of anions, the vibrational modes around 340 cm^{-1} and 530 cm^{-1} are due to bending modes of O-P-O units, PO_2 torsoional (ϵ) vibrations [29, 33], the bands at ~ 750 assigned to symmetric stretching vibrations (v_s) of P–O–P in PO_4 units [30, 33] and v_{as} (P-O-P) at about 915 cm^{-1} [31] in orthophosphate region, the vibrational bands around 1170 cm^{-1} were attributed to symmetric stretch (v_s) mode of $(PO_2)^-$ units in PO_4 tetrahedra [29, 32] and the stretching mode of terminal oxygen (P=O) somewhere in the region ~1280-1380 cm^{-1} ultra-phosphate units [29, 32]. The materials compositions and O/P ratio were tabulated in Table 1.

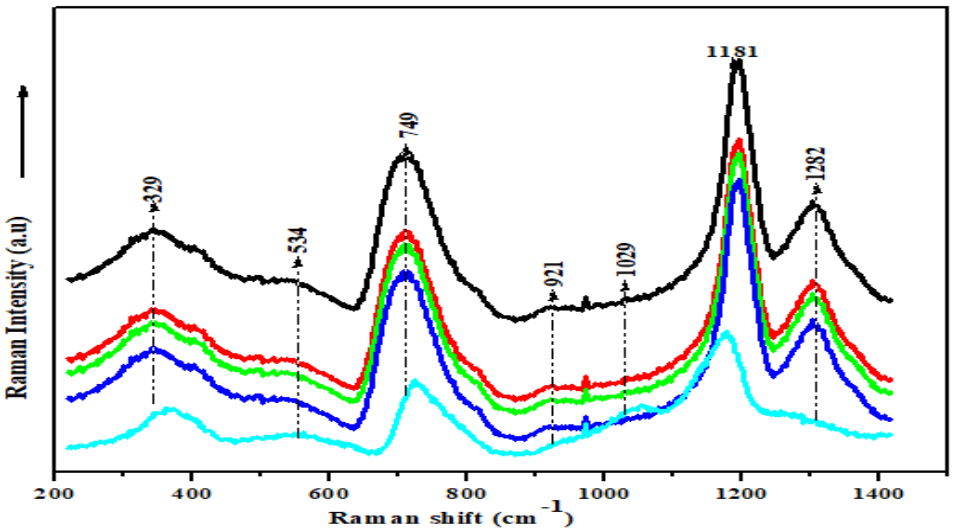

Figure 3 Raman spectra for MSP; Sm glasses

NMR Spectra Analysis

The phosphorus-31 NMR spectra (Figure 4) from different Q-value distribution, two spectral lines were recorded, the isotropic resonance in relation to spinning side-bands signifying the anisotropy of chemical shift. The isotropic peak symbolized by Q^n groups with respect to the chemical shift. The isotropic resonance within the ultra-phosphate (Q^3) region is about –45 ppm, with increase in modifier content the chemical shift in the range of −20 to −30 ppm for meta-phosphate units, is in good agreement with the previous NMR finding [33, 34], 2 clear isotropic contributions are assigned to Q^1,Q^2 units. The spectra are almost similar in shape, with systematic trend move to lower field (taken as the maximum peak) as a result of increase in modifier content. Positive chemical shift are correspond to lower field (downfield) strength while the negative correspond to higher field (up-field) strength. These intermediate bands intensity of the spectra correspond to ultra-, meta- and polyphosphate, other less intense bands occurred in both sides are the spinning side-bands indicated with asterisks, it happens at a result of anisotropies of phosphate species which signifies the anisotropy of chemical shift (CSA). The isotropic shift are indicated by Q^n distribution with respect to the chemical shift (n represent the number of BO per PO_4 tetrahehra) [35**].**

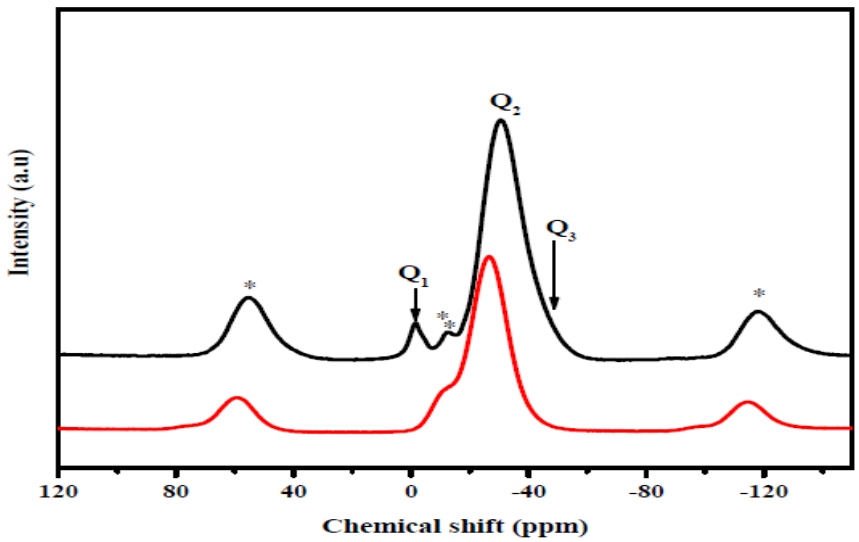

Figure 4 ^{31}P NMR spectra for MSP; Sm glasses

Table 1: Materials composition and O/P ratio

Sample codes	$MgSO_4$	P_2O_5	Sm_2O_3	O/P
MSPSm 1	30	69.8	0.2	3.364
MSPSm 2	30	69.6	0.4	3.370
MSPSm 3	30	69.4	0.6	3.377
MSPSm 4	30	69.2	0.8	3.384
MSPSm 5	30	69.0	1.0	3.391

Physical properties

Density (*ρ)* is the physical properties used to determine the degree of compactivility of materials which are related to the change in geometrical configurations of the sample [36], other physical properties were obtained using molecular weights and density from a suitable expressions such as molar volume (V_m), ion concentration, inter nuclear distance et cetera, the density and refractive index formula as indicated in equations (1 and 2) above. We obtain the rare earth ions concentrations (N_c) as well as the polaron radius (r_p) from following expressions (4 and 5).

$$N_i = \frac{x\rho N_A}{M_T} \quad (4)$$

$$r_p\,(\text{Å}) = \frac{1}{2}\left(\frac{\pi}{6N_i}\right)^{1/3} \quad (5)$$

where N_A is the Avogadro's number, x is the mole fraction of the rare earth ions and M_T is the average molar weight of the samples, the physical properties were tabulated in Table 2. Figure 5 demonstrate the dependence of density and molar volume of the samples, it shows that the density and molar volume changes with increase in Magnesium sulfate content, the trend of the molar volume were directly depends on the density of glasses. There is a decrease in polaron radius with increase in ion concentration (Figure 6), the result found is consistent with [37, 38] inter-nuclear distance decreases with increase in mol % of samarium ions content.

Table 2: Physical properties of the Sm^{3+} doped Magnesium sulfate ultra-phosphate glasses

Physical measurements		Samples				
		0.2%	**0.4%**	**0.6%**	**0.8%**	**1.0%**
Av. molar weight	M(g)	102.108	102.660	102.812	103.312	103.584
Density	ρ (gcm^{-3})	2.3657	2.3901	2.4050	2.4206	2.4420
Molar volume	V_m (cm^3)	43.162	42.952	42.749	42.680	42.418
Sm^{3+} ion concentration	N ($\times 10^{21}$ ion/cm)	2.789	5.606	8.449	11.284	14.192
Polaron radius	r_p (Å) $\times 10^{-8}$	2.863	2.269	1.979	1.797	1.665
Inter-nuclear distance	r_i (Å) $\times 10^{-8}$	7.104	5.629	4.910	4.458	4.130
Field strength	F ($\times 10^{17}$ /cm^2)	0.756	1.205	1.583	1.921	2.238
Refractive index	n	2.159	2.183	2.184	2.188	2.192
Dielectric constant	ε	4.661	4.765	4.770	4.787	4.804
Molar refractivity	R_m (cm^{-3})	23.723	23.910	23.858	23.811	23.716

Molar polarizability	$\alpha_m \times 10^{-24}$	9.405	9.479	9.456	9.459	9.472
Direct mobility gap (eV)	E_{dir} (eV)	4.052	3.941	3.932	3.907	3.886
Indirect mobility gap (eV)	E_{indir} (eV)	4.514	4.538	4.544	4.574	4.512
Width of tail	ΔE (eV)	0.306	0.291	0.224	0.232	0.210

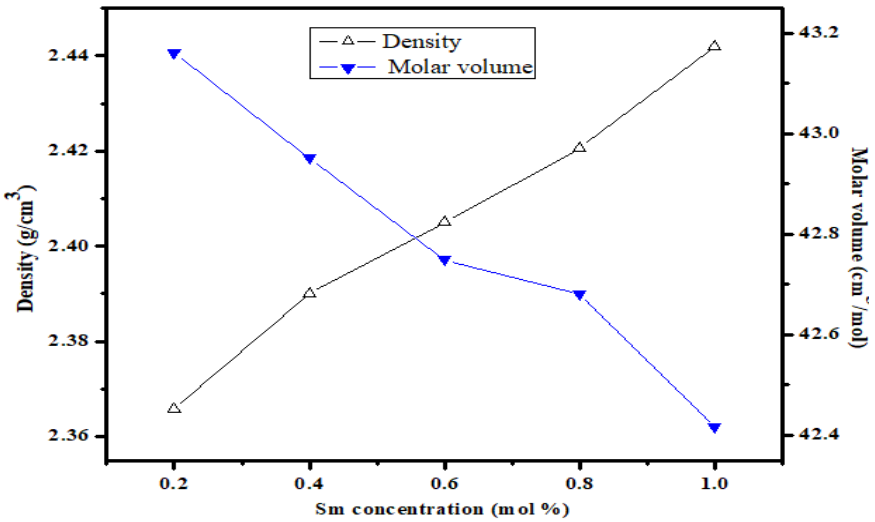

Figure 5: Variation of density against molar volume with increase in mol % of Sm_2O_3 ion.

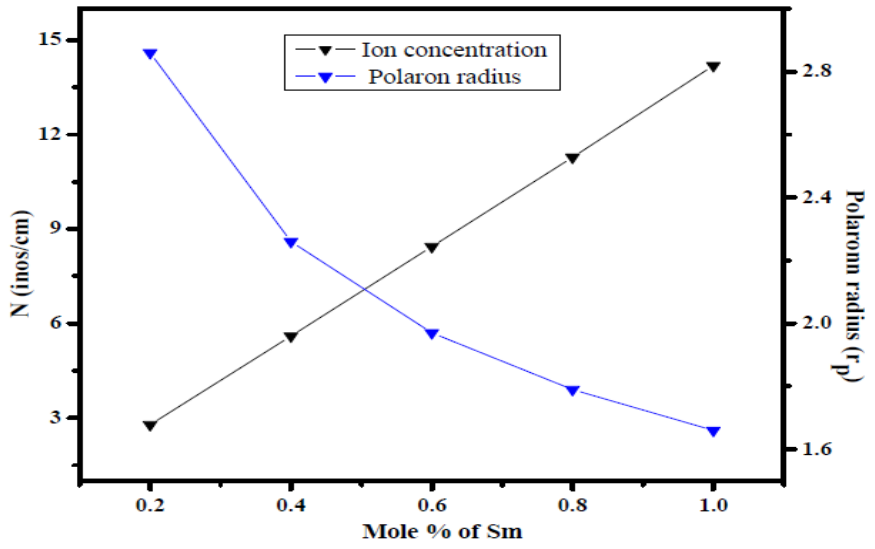

Figure 6: Variation of N (ions/cm) and polaron radius with increase in mol % of Sm_2O_3 ion

Optical absorption spectra

The measured optical absorption spectra for 30MgSO$_4$-(70-*x*) P$_2$O$_5$-*x*Sm$_2$O$_3$, with $0.2 \leq x \leq 1.0$ mol% glasses in the wave length range 350-1800 nm were indicated in Figure 7. The bands were obtained in both glasses as they differ with their intensities. Nine prominent transitions peaks appeared in the UV-Vis-NIR region corresponding to $^6H_{5/2} \rightarrow {}^6P_{3/2}$ $^6H_{5/2} \rightarrow {}^4I_{11/2}$ $^6H_{5/2} \rightarrow {}^6F_{11/2}$, $^6H_{5/2} \rightarrow {}^6F_{9/2}$, $^6H_{5/2} \rightarrow {}^6F_{7/2}$, $^6H_{5/2} \rightarrow {}^6F_{5/2}$, $^6H_{5/2} \rightarrow {}^6F_{3/2}$ $^6H_{5/2} \rightarrow {}^6H_{15/2}$ and $^6H_{5/2} \rightarrow {}^6F_{1/2}$ transition at 400, 472, 945, 1080, 1234, 1380, 1481, 1544 and 1589 nm respectively, the peaks observed are analogous with the other findings [15,39] and the idea of transitions are correspond to carnell *et al* [40].The spectral line is a clear characteristics of *4f–4f* absorption of trivalent Sm_2O_5 corresponds to $^6H_{5/2}$ ground state to an excited states transitions with the energy band positions, the intensities observed changes directly with dopant

(Sm^{3+}) concentration where $^6H_{5/2} \rightarrow {}^6F_{7/2}$ act as the hyper-sensitive transition, the ground state absorption emerge due to ED contributions by obeying the selection rule $|\Delta S| = 0, |\Delta L| \leq 2, and |\Delta J| \leq 2$ [41].

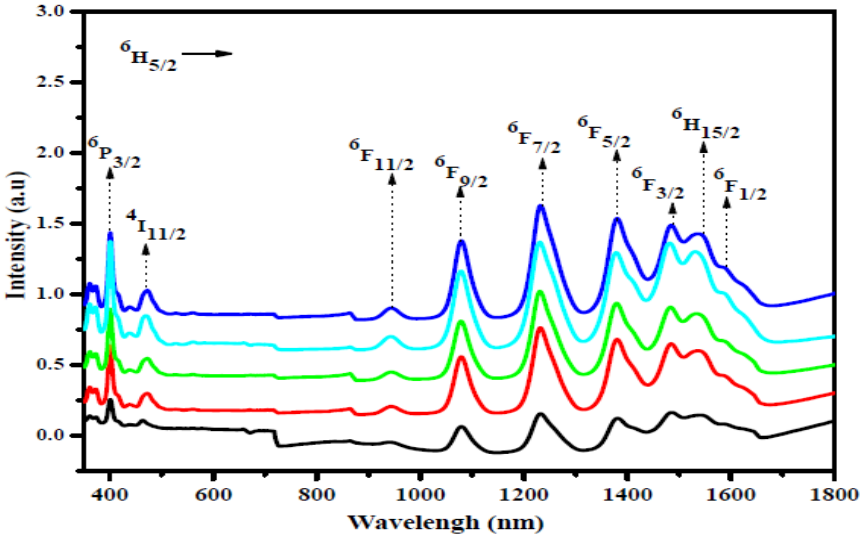

Figure 7: Absorption spectra for$30MgSO_4$-(70-*x*) P_2O_5-*x*Sm_2O_3, with $0.2 \leq x \leq 1.0$ mol% glasses

Band gap energy (ΔE) and Urbach's analysis

The optical band gap values of magnesium sulfate ultra-phosphate glass were obtained through absorption spectra, having two transitions (direct and indirect). From the absorption spectral region, Davis and Mott come up with the following relation for direct and indirect optical transitions is given by

$$\alpha(v) = N(h\nu - E_g^{op})^n / h\nu \quad (6)$$

where the exponent in (6) as n = 2 (indirect allowed) and ½ for allowed direct transitions respectively, N is energy independent constant (band tailing parameter), E_g^{op} is optical band gap of *hv* as photon energy of incident radiation (Tauc's gap), the scheme of $(\alpha h\nu)^{1/2} = 0$ and $(\alpha h\nu)^2 = 0$ for indirect and the direct allowed transitions [42], The E_g^{op} energies can be obtained from (6) by extrapolating the absorption coefficient to zero absorption, the dependency of $(\alpha h\nu)^2$ on *hv* have been plotted as in Figure 6(a). The E_g^{op} value decreases with increase in samarium ion content, where the modifier addition contribute to the change in phosphate structure, this may also lead to decrease in optical band gap [43] the increase in NBOs indicates the upturn of free electrons and result in the decreasing number of optical band gap energy [44]. It was discovered that the increase in dopant content may improve the degree of localization there by creating defects in the charge distribution; as such, the energy of the nearest oxygen ions were induced to the top valence band to raised the number of donor centers of the system. The upward turn in donor centers causes the downturn in the band gap energy values [45]. The Urbach energy (ΔE) provides an information about the disorderliness between the host and impurities atoms, when high energy UV light is absorbed by the glassy phases, the values obtained were evaluated by taking the inverse of the slopes of ln α versus photon energy as presented in Figure 6(b), the band tails are represented by a band tail parameter, ΔE, (Urbach energy) given by [40]

$$\alpha(v) = \beta \exp\left(\frac{hv}{\Delta E}\right) \quad (7)$$

where is β constant referred to band tailing parameter and ΔE is the Urbach energy interpreted as the width of the localized tail state in the optical band gap, the urbach energy values were listed in Table 2.

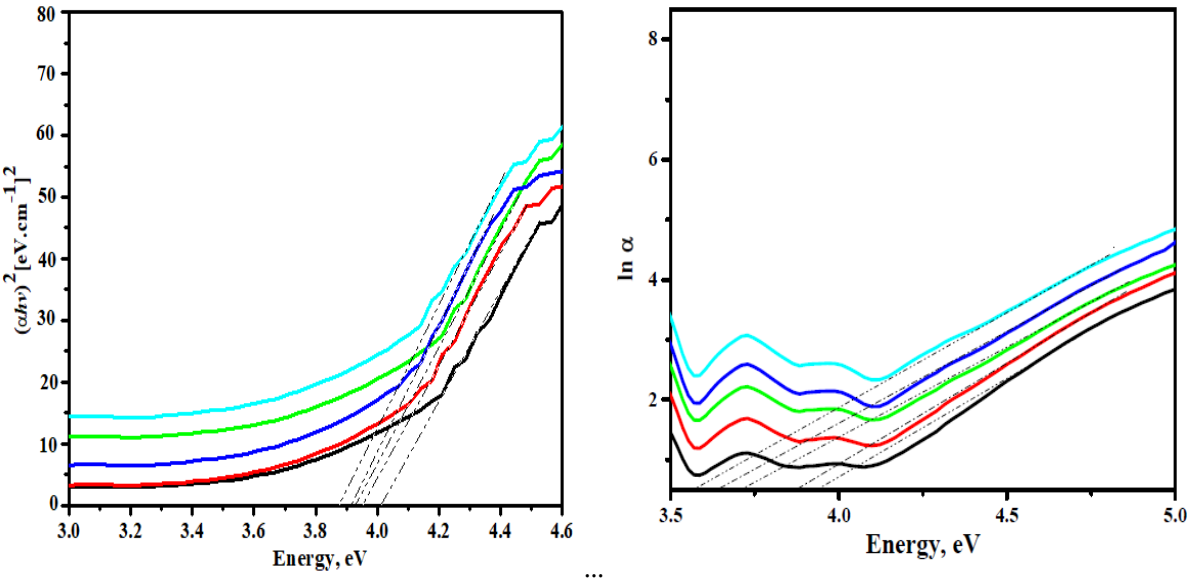

Figure 6: (a) Optical band gap for MSP; Sm glasses **(b)** Urbach energy for MSP; Sm glasses

DISCUSSION

Phosphate based glasses (PBGs) constitute of an inorganic phosphate network (as P_4^{3-} tetrahedral units serves as main building block). In *v*-Phosphate, the phosphorus (P) and oxygen (O) atoms are configured in 3-D polymerized network structure of rings and chains, the tertahedra is link to adjacent units by 3 of 4 vertices where the fourth side is occupied by double-bond oxygen atom [46].The tetrahedra (P_4^{3-}) are formed by sp^3 hybridization of P outer-shell electrons (as $3s^2$ $3p^3$), this tetrahedra units are expressed in terms on Q^n nomenclature (n represent the number of BOs per phosphate tetrahedtra. The network structure is strongly depends on the modifier oxide content, the condensed phosphate Q^n groups are ultra-phosphate, Q^3 (branching unit), meta-phosphate, Q^2 (middle unit), poly-phosphate, Q^1(end unit) and ortho-phosphate unit, Q^0 (isolated tetrahedtra), the Q^3 (branching unit) react with modifier oxides to form Q^2 (middle unit), all Q species depend on the O/P ratio in accordance to stoichiometry refer to Table 1. Incorporation of modifier oxide (MgO) to phosphate effect the phosphate link to formed P-O-K (K= metal ion), hence de-polymerized the structure. The quantitative measurements of Q^n distribution are in consistent with the Van Wazar predictions for the structure of phosphate [47]. Van Wazar formalized the transformation of P_2O_5 structures with increase or decrease in compositions. The embedded modifier oxides (MgO in %) can be schematically represented by modifier pseudo-reaction according to $2Q^n + R_2O \rightarrow Q^{n-1}$ where R_2O or RO are the monovalent or divalent cations. In terms Q^3 branching units the modifier react to form Q^2 species (as $2Q^3 + R_2O \rightarrow 2Q^2$) hence, the number of NBOs increases. The degree of phosphate polymerizations were express by the relative amount of modifier content which described in term of elementary structural units ultra-, Q^3 $(POO_{3/2})^0$, meta-,Q^2 $(POO_{2/2}O)^-$, poly- Q^1 $(POO_{1/2}O_2)^{2-}$ and ortho-phosphate,

Q^0 $(POO_{0/2}O_3)^{3-}$ respectively. The interaction of $[POO_{2/2}O]^-$ ions with sulfate to form SPO_7^{3-} (dithiophophate) species [10, 47].The small fraction of phosphate tetrahedra (PO_4) may associate with ring structures which limit the chain length [33], but the development of phosphate rings does not affect the Q^n distribution. It is worth considering that, the atomic arrangements in the short and intermediate range of networks are the most significant factor that determines the emission feature of the materials. The covalency/or symmetry of rare earth ions are different when modifier oxides are merge between the longer chain of RE ions in S-O-P network. Likewise, the differences in the structure of phosphate and sulfate ions with respect to their concentration change the crystal field around the lanthanides ions in the samples [48]. The relative MgO content cannot be obtain by the NMR spectra, however, the region of Q^n distribution of ultra-, meta- and orthophosphates region with their ratio remain valid [34] in both FTIR, Raman and NMR specta..

CONCLUSION

The average order of phosphate chains in the magnesium sulfate ultra-phosphate glasses becomes increasingly shorter as the modifier ($MgSO_4$) content is gradually increased. The process is quantitatively expressed by the increasing concentration of pyro-phosphate (Q^1) and ortho-phosphate (Q^0) groups determined by FTIR and Raman spectra with different degrees of polymerization were easily resolve by NMR in Q^1,Q^2 and Q^3 units . The experiments indicate the progressive de-polymerization of phosphate structure, the structure of the glass samples becomes more compressed, and this attributed to the increasing connectivity of $MgSO_4$ and the samarium ions content by sharing the NBOs atoms leading to the reduction of the space distances, The increasing trend of ρ (density) due to increase in Sm^{3+} oxide content with decrease in molar volume result in decrease in the bond length on the inter atomic spacing in between the atoms The refractive index (RI) increases with increase of dopant owing to decrease in optical energy gap. From the optical analysis, we concluded that upturn of samarium oxides results in decrease of optical energy gap attributed to increase in NBOs ions. The absorption spectra affirm that the fundamental absorption edge shifts to higher wavelength as the dopant content increases. Optical band gap (direct and indirect) and Urbach are found in ranges, the dependence of α (*v*) on *h*v obeys the Urbach rule. Our studies confirmed the stability and suitability of the materials in the progress of optical laser materials.

Acknowledgement

We would like to express our gratitude to Ministry of Higher Education Malaysia and UTM for their financial support through the FRGS of the Vote number (QJ130000.2526.01H01) and also appreciate the effort of Bauchi State University, Gadau Nigeria.

REFERENCE

[1] M. Abid, M. Et-tabirou, M. Taibi, Structure and DC conductivity of lead sodium ultraphosphate glasses, Mater. Sci. Eng. B 97 (2003) 20-24

[2] S.F. Ismail, M.R. Sahar, S.K. Ghoshal, Physical and absorption properties of titanium nano-particles incorporated into zinc magnesium phosphate glass, Mater. Charact**.** 111 (2016) 177-182

[3] R. Praveena, V. Venkatramu, P. Babu, C.K. Jayasankar, Fluorescence spectroscopy of Sm^{3+} ions in P_2O_5- PbO-Nb_2O_5 glasses, Physica B 403 (2008) 3527- 3534

[4] Bin Qian, Xiaofeng Liang, Shiyuan Yang, Shu He, Long Gao. Effects of lanthanum addition on the structure and properties of iron phosphate glasses, J. Mol. Struct. 1027 (2012) 31-35

[5] Toshinori Okura, Tomoko Miyachi, Hideki Monma, Properties and vibrational spectra of magnesium phosphate glasses for nuclear waste immobilization, J. Eur. Ceram. Soc**.** 26 (2006) 831-836

[6] N. Sooraj Hussain, M.A. Lopes, J.D. Santos, A comparative study of CaO-P_2O_5-SiO_2 gels prepared by a sol-gel method, Mater. Chem. Phys 88 (2004) 5-8

[7] Yasser B. Saddeek, Network structure of molybdenum lead phosphate glasses: Infrared spectra and constants of elasticity**,** Physica B 406 (2011) 562-566

[8] Daniela Carta, David M. Pickup, Jonathan C. Knowles, I. Ahmed, Mark E. Smith, Robert J. Newport, A structural study of sol-gel and melt-quenched phosphate-based glasses, J. Non-Cryst. Solids 353 (2007) 1759-1765

[9] R. Hussin, Muhammad Shawal Husin, Dayang Nur Fazliana Abdul Halim and Sinin Hamdan, Vibrational studies of crystalline phase strontium magnesium phosphates doped with Eu_2O_3, Adv. Mater. Res. 18 (2010) 288-301

[10] F Ahmadi1, R Hussin and S K Ghoshal, Structural and physical properties of Sm^{3+} doped magnesium zinc sulfophosphate glass, Bull. Mater. Sci,40 (2017) 1097-1104

[11] A. M. Aliyu, R. Hussin, Karim Deraman, N. E. Ahmad, Amina M. Danmadami, Y. A. Yamusa, Physical and optical properties of calcium sulfate ultra-phosphate glass-doped Er_2O_3, Int. J. M. P. B,32 (2018) 1-14

[12] M.A. Karakassides, A. Saranti, I. Koutselas, Preparation and structural study of binary phosphate glasses with high calcium and/or magnesium content, J. Non-Cryst. Solids 347 (2004) 69-79

[13] G. Walter, J. Vogel, U. Hoppe, P. Hartmann, Structural study of magnesium polyphosphate glasses, J. Non-Cryst Solids 320 (2003) 210-222

[14] E. Matsubara, Y. Waseda, M. Ashizuka, E. Ishida, Structural study of binary phosphate glasses with MgO, ZnO, and CaO by X-ray diffraction, J. Non-Cryst. Solids 103 (1988) 117-124

[15] Yasser Saleh Mustafa Alajerami, Suhairul Hashim, Wan Muhamad Saridan Wan Hassan, Ahmad Termizi Ramli, Azman Kasim, Optical properties of lithium magnesium borate glasses doped with Dy^{3+} and Sm^{3+} ions, Physica B 407 (2012) 2398-2403

[16] Simon Striepe, Ning Da, Joachim Deubener, Lothar Wondraczek, Micromechanical properties of (Na,Zn)-sulfophosphate glasses, J. Non-Cryst. Solids 358 (2012) 1032-1037

[17] Arnulf Thieme, Doris Möncke, René Limbach, Sindy Fuhrmann, Efstratios I. Kamitsos, Lothar Wondraczek, Structure and properties of alkali and silver sulfophosphate glasses, J. Non-Cryst. Solids 410 (2015) 142–150

[18] T.G.V.M. Rao, A.Rupesh Kumar, N. Veeraiah, M.Rami Reddy, Optical and structural investigation of Sm^{3+} –Nd^{3+} co-doped in magnesium lead boro-silicate glasses, J. Phy. Chem. Solids 74 (2013) 410–417

[19] P. Raghava Rao, G.MuraliKrishna, M.G.Brik, Y.Gandhi, N.Veeraiah. Fluorescence features of Sm^{3+} ions in Na_2SO_4-MO-P_2O_5 glass system Influence of modifier oxide, J. lumin. 131 (2011) 212- 217

[20] Z. Mazurak, S. Bodył, R. Lisiecki, J. Gabrys´-Pisarska, M. Czaja, Optical properties of Pr3+, Sm^{3+} and Er^{3+} doped P_2O_5-CaO-SrO-BaO phosphate glass, Opt. Mater. 32 (2010) 547-553

[21] C.R. Kesavulu, C.K. Jayasankar, White light emission in Dy^{3+} -doped lead fluorophosphate glasses, Mater. Chem. Phy. 130 (2011) 1078 - 1085

[22] Ki-Soo Lim, N. Vijaya, C.R. Kesavulu, C.K. Jayasankar, Structural and luminescence properties of Sm^{3+} ions in zinc fluorophosphate glasses, Opt. Mater. 35 (2013) 1557-1563

[23] V. Venkatramu, P. Babu, C.K. Jayasankar, Th. Tro¨ ster, W. Sievers, G. Wortmann, Optical spectroscopy of Sm^{3+} ions in phosphate and fluorophosphate glasses, Opt. Mater. 29 (2007) 1429-1439

[24] P. Chimalawong, J.Kaewkhao, C.Kedkaew, P.Limsuwan, Optical and electronic polarizability investigation of Nd^{3+} -doped soda-lime silicate glasses, J. Phy. Chem. Solids 71 (2010) 965-970

[25] C. Dayanand, G. Bhikshamaiah, V. Jayatyagaraju, M. Salagram, Review structural investigations of phosphate glasses: a details infrared study of the *x* (PbO)- (1-*x*) P_2O_5 vitreous system, J Mater Sci 31 (1996) 1945-1967

[26] A. A. Higazy and B. Brigde, Infrared spectra of vitreous system Co_3O_4-P_2O_5 and their interpretation, J Mater Sci 20 (1985) 2345-2358

[27] H. Doweidar, Y.M. Moustafa, K. El-Egili, I. Abbas, Infrared spectra of Fe_2O_3-PbO-P_2O_5 glasses, Vib Spectrosc 37 (2005) 91-96

[28] M. Sherief. Abo-Naf, N. A. Ghoneim, H. A. El-Batal, Preparation and characterization of Sol-gel derived glasses in the ternary Na_2O-Al_2O_3-P_2O_5 system, J. Mater. Sci-Mater El, 15 (2004) 273-282

[29] L. Baia, D. Muresan, M. Baia, J. Popp, S. Simon, Structural properties of silver nano-clusters phosphate glass composite, Vib. Spectrosc. 43 (2007) 313-318

[30] M. Hafid, T. Jermoumi, N. Toreis, T. Ghailassi, Structure of (45-*x*) Na_2O-*x*BaO-5ZnO-50P_2O_5 glasses studied by DSC and infrared spectroscopy, Mate. Lett**,** 56 (2002) 486-490

[31] P. Raghava Rao, L. Pavić, A. Moguš-Milanković, V. Ravi Kumar, I.V. Kityk, N. Veeraiah, Electrical and spectroscopic properties of Fe_2O_3 doped Na_2SO_4-BaO-P_2O_5 glass system, J. Non-Cryst. Solids 358 (2012) 3255-3267

[32] J. Schwarz, H. Tichá, L. Tichý, R. Mertens, Physical properties of PbO-ZnO-P_2O_5 glasses I. Infrared and Raman spectra, J. Optoelectron. Adv. M, 6 (2004) 737 - 746

[33] R. K. Brow, R. J. Kirkpatrick, & G. L. Turner, The short range structure of sodium phosphate glasses I. MAS NMR studies. J. Non-Cryst Solids, 116 **(**1990**)** 39-45.

[34] H. Aguiar, E.L. Solla, J. Serra, P. González, B. León, F. Malz, C. Jäger, Raman and NMR study of bioactive Na_2O–MgO–CaO–P_2O_5–SiO_2 glasses, J. Non-Cryst Solids 354 (2008) 5004–5008

[35] R. K. Brow, D. R. Tallant, J. J. Hudgens, S. W. Martin, & A. D. Irwin, The short-range structure of sodium ultraphosphate glasses. J. Non-Cryst Solids, 177 (1994) 221-228.

[36] M. F. Faznny, M. K. Halimah, M. N Azlan, Effect of lanthanum oxide on optical properties of zinc boro-tellurite glass system, J. Optoelectron Bio Mater 8 (2016) 49 - 59

[37] S. Mohan, K. S. Thind, and G. Sharma, Effect of Nd^{3+} Concentration on the Physical and Absorption Properties of Sodium-Lead-Borate Glasses, Brazil J. Phy, 37(2007) 1306-1313

[38] K. El-Egili, H. Doweidar, Y.M. Moustafa, I. Abbas, Structure and some physical properties of PbO–P_2O_5, Physica B 339 (2003) 237–245

[39] T. Suhasini, J. Suresh Kumar, T. Sasikala, Kiwan Jang, Ho Sueb Lee, M. Jayasimhadri, Jung Hyun Jeong, Soung Soo Yi, L. Rama Moorthy, Absorption and fluorescence properties of Sm^{3+} ions in fluoride containing phosphate glasses, Opt. Mater. 31 (2009) 1167–1172

[40] W. Carnall, P. Fields and K. Rajnak, Electronic energy levels in the trivalent lanthanides Aquo ions I. Pr^{3+}, Nd^{3+}, Pm^{3+}, Sm^{3+}, Dy^{3+}, Ho^{3+}, Er^{3+}, and Tm^{3+} J. Chem. Phys. 49 (1968) 4424-4442

[41] S. Surendra Babu, P. Babu, C.K. Jayasankar, Th. Tröster, W. Sievers, G. Wortmann, Optical properties of Dy^{3+} doped phosphate and fluorophosphate glasses, Opt. Mater. 31 (2009) 624–631

[42] Manal Abdel-Baki, F.A. Abdel-Wahab, Amr Radi, Fouad El-Diasty, Factors affecting optical dispersion in borate glass systems, J. Phy. Chem. Solids 68 (2007) 1457-1470

[43] S. Sindhu, Sanghi S., Argawal A., Sonam S.V.P., Kishore N, The role of V_2O_5 in the modification of structural, optical and electrical properties of vanadium barium borate glasses, Physica B, 365 (2005), 65

[44] A. Awang, S.K. Ghoshal, M.R. Sahar, M. Reza Dousti, Raja J. Amjad, Fakhra Nawaz, Enhanced spectroscopic properties and Judd-Ofelt parameters of Er-doped tellurite glass: Effect of gold nano-particles, Curr Appl Phys 13 (2013) 1813-1818

[45] M.H.A.Mhareb, S.Hashim, S.K.Ghoshal, Y.S.M.Alajerami, M.J.Bqoor, A.I.Hamdan, M.A.Saleh, M.K.B.AbdulKarim, Effect of Dy_2O_3 impurities on the physical, optical and thermo-luminescence properties of lithium borate glass, J. Lumin. 177 (2016) 366-372

[46] N. Sharmin, & C. D. Rudd, Structure, thermal properties, dissolution behaviour and biomedical applications of phosphate glasses and fibres: a review. J. Mater Sci 52 (2017) 8733-8760

[47] A.V. Ravi Kumar, Ch. Srinivasa Rao, T. Srikumar, Y. Gandhi, V. Ravi Kumar, N. Veeraiah, Dielectric dispersion and spectroscopic investigations on Na_2SO_4–B_2O_3–P_2O_5 glasses mixed with low concentrations of TiO_2, J. of Alloys Compd. 515 (2012) 134– 142